

Defence Science Journal, Vol. 59, No. 2, March 2009, pp. 113-125
© 2009, DESIDOC

Tracking the Warhead Among Objects Separation from the Reentry Vehicle in a Clear Environment

Cheng-Yu Liu and Chi-Teh Chen

Lee-Ming Institute of Technology, Taipei, Taiwan, R.O.C.

ABSTRACT

Separating a reentry vehicle into warhead, main body, and debris is a conventional and efficient means of producing a huge decoy and increasing the kinetic energy of the warhead. This procedure causes the radar to track the main body and debris, which radar cross section are large, and ignore the warhead, is the most important part of the reentry vehicle. The warhead is difficult to identify after separation using standard tracking criteria. This study presents a novel tracking algorithm by integrating input estimation and modified probabilistic data association filter to identify warhead among objects separation from the reentry vehicle in a clear environment. The proposed algorithm provides a good tracking capability for the warhead ignoring the radar cross section. Simulation results reveal that the errors between the updated and warhead trajectories are reduced to a small interval in a short time. Therefore, the radar can generate a beam to illuminate the right area and keep tracking the warhead all the time. This algorithm is worthy of further study and application.

Keywords: Input estimation, probabilistic data association filter, extended Kalman filter, tracking algorithm, trajectory estimation

NOMENCLATURE

C	Ballistic coefficient for the RV (kg/m^2)
C_i	Ballistic coefficient for the i -th object (kg/m^2)
C_{D0}	Zero-lift drag coefficient
e_i	Length of the normalized innovation in position for the i -th candidate
g	Gravity (m/s^2)
$G(i)$	6×6 gain matrix
$I_{n \times n}$	$n \times n$ identity matrix
$K(n+1)$	6×6 Kalman gain matrix
$K_i^v(n+1)$	6×6 Kalman gain matrix with the estimated input for the i -th object
N	Number of objects separation from the RV
$P(k+l+1 k+l)$	6×6 covariance matrix of the predicted states for the EKF with no input
P_z	6×6 variance matrix of $\hat{Z}(k+l)$
Q	6×6 covariance matrix of process noise
Q_i	6×6 covariance matrix of process noise for the i -th object
R	6×6 covariance matrix of measurement noise
S	Reference area of the RV (m^2)
$V(i)$	6×6 covariance matrix of the estimated input
W	Weight of the RV (kg)
$\hat{Z}(k+l)$	Unmodeled inputs in X_R , Y_R and Z_R , respectively (m/s^2)
u_{ix}, u_{iy}, u_{iz}	Unmodeled inputs in X_R , Y_R and Z_R , respectively

v, v_i	Total velocities for the RV and the i -th object (m/s)
v_x, v_y, v_z	Velocity components (m/s)
x, y, z	Positions (m)
$Z(n+1)$	Measurements at $t = (n+1)\Delta t$
$\hat{Z}(k+l)$	Measurement residual for the EKF formation with inputs
Z^{n+1}	Measurement vector collecting the measurements from $t = 0$ to $t = (n+1)\Delta t$
$0_{n \times n}$	$n \times n$ zero matrix
Δt	Sampling period (s)
ρ	Air density (kg/m^3)
ζ	6×1 process noise vector
ζ_i	6×1 process noise vector for the i -th object
ε	6×1 measurement noise vector
γ_1, γ_2	Elevation and flight path angles for the RV, respectively
γ_{i1}, γ_{i2}	Elevation and flight path angles for the i -th object, respectively

1. INTRODUCTION

Separation of the reentry vehicle (RV) into several objects, including the warhead, main body, and debris during the reentry phase, is an effective means of confusing radar by generating many sets of measurements from a radar beam. The radar estimates and predicts the target trajectory at the next sampling

Received 1 January 2008

period from the measurement with the highest signal-to-noise ratio and forms a beam to illuminate it. The body or debris is then tracked and intercepted first, since its radar cross section is inevitably larger than that of the warhead. The warhead, which is the most significant part of the RV, then becomes a new track or is completely disregarded. This problem is hard to solve unless the standard tracking criterion is modified.

Two issues, estimation of warhead trajectory and origination of measurements, have been introduced to solve this problem. If a warhead does not alter its trajectory in separation, then it typically follows the original trajectory closely. However, the body and debris fall down faster than the warhead in random directions. Then, the residual wrt the warhead, given by the difference between the estimated and real warhead trajectories, is smaller than that wrt the other objects. An online precision trajectory estimation approach is required. Data association technique can be adopted to solve the origination problem.

The main problems with the online estimation of the RV trajectory relate to model validation, owing to model error between the mathematical model and the physical system. The model error is normally the result of the simplifying assumptions, manoeuvring and unpredictable external forces during flight or parameter uncertainty. The extended Kalman filter (EKF) is a well-known and helpful state estimation scheme for a nonlinear dynamic system, but fails to reach the required accuracy in a short time. Input estimation (IE) provides a good solution to this problem. IE has been successfully employed to estimate inputs for solving tracking¹⁻⁴, inverse heat conduction⁵⁻⁷ and initial leveling problems^{8,9}. Lee and Liu proposed a filter associating the EKF with IE to handle model validation problems, and provided an accurate trajectory estimation approach for the RV¹⁰⁻¹⁴. Their proposed filter has lower estimation errors than the original EKF, and is helpful for this problem.

Bar-Shalom designed a suboptimal Bayesian algorithm, probabilistic data association filter (PDAF)^{15,16}, for tracking a single target in a cluttered environment. It combines the states of all radar returns weighted by a *a posteriori* probability, known as association probability, to form the combined states of the target. The PDAF has been successfully utilised in sonar and radar systems to increase their tracking capacity^{17,18}. A modified PDAF (MPDAF) with a new defined association probability has also been developed. MPDAF links with the EKF and IE to create a tracking algorithm for clarifying warhead between two objects split from the RV in a clear environment¹⁹. This algorithm enables the radar to identify the warhead in a few seconds following separation, and could be used to track warhead in a complex situation.

This investigation presents a novel algorithm by inserting an identification procedure on the MPDAF to detect the warhead among more than two objects split from the RV in a clear environment.

2. DYNAMIC EQUATIONS

Define the radar Cartesian coordinate system to be centred at the radar site O_R with three axes downrange X_R , off-range Y_R , and altitude Z_R .

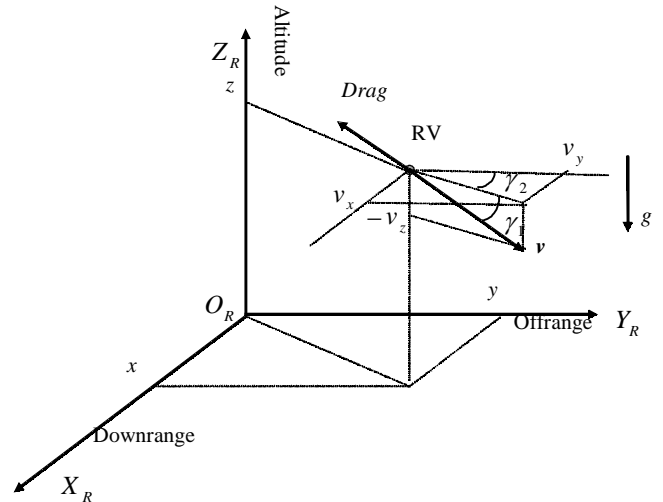


Figure 1. Reentry vehicle flight geometry

Figure 1 shows a vehicle in the reentry phase over a flat and nonrotating earth. Assume the RV is a point mass with constant weight following a ballistic trajectory in which two significant forces, drag and gravity, act on the RV. Extra forces are induced by model error when assumptions are violated or the RV undertakes a manoeuvre. The RV trajectory model can be written as²⁰

$$\dot{v}_x = -\frac{\rho v^2}{2C} g \cos \gamma_1 \sin \gamma_2 + u_x \quad (1)$$

$$\dot{v}_y = -\frac{\rho v^2}{2C} g \cos \gamma_1 \sin \gamma_2 + u_y \quad (2)$$

$$\dot{v}_z = -\frac{\rho v^2}{2C} g \sin \gamma_1 - g + u_z \quad (3)$$

with position initial conditions $x(0), y(0), z(0)$ and velocity initial conditions $v_x(0), v_y(0), v_z(0)$ in X_R, Y_R and Z_R , respectively. In this model,

$$C = \frac{W}{SC_{D0}}$$

$$\gamma_1 = \tan^{-1} \left(-\frac{v_z}{\sqrt{v_x^2 + v_y^2}} \right) \quad \gamma_2 = \tan^{-1} \left(\frac{v_z}{v_y} \right)$$

ρ stands for air density and is a function of altitude²⁰

$$\rho(z) = 0.002378e^{-z/30000} \quad \text{for } z < 30000 \text{ ft} \quad (4)$$

$$\rho(z) = 0.0034e^{-z/22000} \quad \text{for } z \geq 30000 \text{ ft} \quad (5)$$

The well known normal gravity g model is extensively used²¹. Among these parameters, C is the key parameter and is the only parameter unknown to radar. To estimate RV's position and velocity, the EKF with augmented state C may solve this problem. However, C is unmeasurable from a radar and would worsen the estimation results seriously. C is thus be assumed to be a constant during entire operating envelope for simplicity.

Let the state vector be

$$\begin{aligned} X(t) &= [x_1 \ x_2 \ x_3 \ x_4 \ x_5 \ x_6]^T \\ &= [x \ y \ z \ v_x \ v_y \ v_z]^T \end{aligned} \quad (6)$$

The nonlinear state equation can be written as

$$\dot{X}(t) = F(X) + \varphi u + \zeta \quad (7)$$

$$F(X) = \begin{bmatrix} x_4 \\ x_5 \\ x_6 \\ -\frac{\rho}{2C_b}(x_4^2 + x_5^2 + x_6^2)g \cos \gamma_1 \sin \gamma_2 \\ -\frac{\rho}{2C_b}(x_4^2 + x_5^2 + x_6^2)g \cos \gamma_1 \cos \gamma_2 \\ \frac{\rho}{2C_b}(x_4^2 + x_5^2 + x_6^2)g \sin \gamma_1 - g \end{bmatrix} \quad \varphi = \begin{bmatrix} 0_{3 \times 3} & 0_{3 \times 3} \\ 0_{3 \times 3} & I_{3 \times 3} \end{bmatrix}$$

The precision phased array radar, i.e., a digital radar is used in tracking, and is the only instrument in the system for detecting RV. The detected elevation, azimuth, and range are transferred into position in Cartesian frame. Since the detected velocity measured from pulse Doppler did not meet the accuracy needs, the velocity obtained by a specific filter in radar is taken as the measurements to improve estimation accuracy. If the filter is taken into account, a nonlinear measurement equation is involved and becomes too complicated to be accomplished. For simplicity and being implemented easily, the effect of nonlinearity induced by filtering is ignored and left to the future study. The linear measurement equation for the RV is then given by

$$Z(t) = X(t) + \varepsilon(t) \quad (8)$$

where ε denotes the measurement noise vector, which is assumed to be normally distributed with mean zero and variance R . Equations (7) and (8) are the dynamic equations for the RV during reentry.

The RV separates into N objects, including the warhead, body and debris, at $t = t_s$. The warhead generally flies along a slightly different trajectory from that of the original RV if no action is conducted. The body and debris then deviate from the original RV trajectory, and fall on their own. Equations of motion for each object with the ballistic coefficient C_p , $i = 1, 2, \dots, N$, after separation can be expressed as

$$\dot{v}_{ix} = -\frac{\rho v_i^2}{2C_i} g \cos \gamma_{i1} \cos \gamma_{i2} + u_{ix} \quad i = 1, 2, \dots, N \quad (9)$$

$$\dot{v}_{iy} = -\frac{\rho v_i^2}{2C_i} g \cos \gamma_{i1} \cos \gamma_{i2} + u_{iy} \quad i = 1, 2, \dots, N \quad (10)$$

$$\dot{v}_{iz} = \frac{\rho v_i^2}{2C_i} g \sin \gamma_{i1} - g + u_{iz} \quad i = 1, 2, \dots, N \quad (11)$$

with position initial conditions $x_i(t_s), y_i(t_s), z_i(t_s)$ and velocity initial conditions $v_{ix}(t_s), v_{iy}(t_s)$, and $v_{iz}(t_s)$ in X_R, Y_R and Z_R respectively.

Let the state vector for the i -th object to be

$$X_i(t) = [x_{i1} \ x_{i2} \ x_{i3} \ x_{i4} \ x_{i5} \ x_{i6}]^T = [x_i \ y_i \ z_i \ v_{ix} \ v_{iy} \ v_{iz}]^T \quad (12)$$

The nonlinear state equation can be written as

$$\dot{X}_i(t) = F(X_i) + \varphi u_i + \zeta_i \quad t > t_s \quad (13)$$

where $u_i = [0 \ 0 \ 0 \ u_{ix} \ u_{iy} \ u_{iz}]^T$

The measurement equation for the i -th object is then given by

$$Z_i(t) = X_i(t) + \varepsilon(t) \quad t > t_s \quad (14)$$

3. EXTENDED KALMAN FILTER WITH INPUT ESTIMATION

The input estimation algorithm estimates unknown inputs in state equations from pseudo-residuals. At $t \leq t_s$, the predicted and updated state vectors of the RV by the EKF from $t = n\Delta t$ to $t = (n+1)\Delta t$, $n = 0, 1, 2, \dots$, under input vector $u(n)$ at $t = n\Delta t$ are given by, respectively²²

$$\hat{X}(n+1|n+1) = \hat{X}(n+1|n) + K(n+1) \quad (15)$$

$$\hat{X}(n+1|n+1) = \hat{X}(n+1|n) + K(n+1)$$

$$\left[Z(n+1) - \hat{X}(n+1|n) \right] \quad (16)$$

where $\varphi_\Delta = \varphi \Delta t$ and let $\bar{X} = (n+1|n+1)$ denote the updated state for the EKF with no input at $t = (n+1)\Delta t$. For simplicity, let $\hat{X}(n+1) = \hat{X}(n+1|n+1)$ and $\bar{X}(n+1) = \bar{X}(n+1|n+1)$. Define

$$M(n+1) = [I - K(n+1)]\varphi(n) \quad (17)$$

$$N(n+1) = [I - K(n+1)]\varphi_\Delta \quad (18)$$

Assume that the abrupt deterministic inputs are applied during $k\Delta t \leq t \leq (k+s)\Delta t$,

$$u = \begin{cases} 0 & t < k\Delta t, t > (k+s)\Delta t \quad k, s > 0 \\ u(k+l) & k\Delta t \leq t \leq (k+s)\Delta t \quad l = 0, 1, 2, \dots, s \end{cases} \quad (19)$$

where $u(k+l)$ is a constant vector over the sampling interval. Then, $\hat{X}(k) = \bar{X}(k)$ during $t \leq k\Delta t$. The difference induced by the abrupt inputs between these two formations during $k\Delta t \leq t \leq (k+s)\Delta t$ can then be written as

$$\begin{aligned} \Delta X(k+l) &= \hat{X}(k+l) - \bar{X}(k+l) \\ &= M(k+l)\Delta X(k+l-1) + N(k+l)u(k+l-1) \end{aligned} \quad (20)$$

Define the measurement residual for the EKF formation without and with inputs to be $\bar{Z}(k+l) = Z(k+l) = \bar{X}(k+l)$ and $\hat{Z}(k+l) = Z(k+l) = \hat{X}(k+l)$, respectively. The recursive least-squares input estimator can be derived as¹⁰

$$\begin{aligned} \hat{u}(k+l-1) &= \hat{u}(k+l-2) + G(k+l) \\ &\quad \left[\hat{Y}(k+l) - N(k+l)\hat{u}(k+l-2) \right] \end{aligned} \quad (21)$$

where

$$\hat{Y}(k+l) = \bar{Z}(k+l) - M(k+l)\Delta \hat{X}(k+l-1)$$

$$\begin{aligned}\Delta\hat{X}(k+l-1) &= M(k+l)\Delta\hat{X}(k+l-2) + N(k+l)\hat{u}(k+l-2) \\ G(k+l) &= V(k+l-1)N(k+l)P_z^{-1} \\ V(k+l-1) &= V(k+l-2) - V(k+l-2)N(k+l)^T \\ &\quad \times [N(k+l)V(k+l-2)N(k+l)^T + P_z]^{-1} \\ &\quad \times N(k+l)V(k+l-2) \\ P_z &= R + P(k+l+1|k+l)\end{aligned}$$

In Eqn. (19), k and $k+s$ respectively denote the starting and stopping indices of the system input, which can be obtained by testing. Two hypotheses, existence and absence of inputs, are set. Each normalised estimated input at time $k+l-1$ locates on the confidence interval $[-t_{st}, t_{st}]$ if the first hypothesis is satisfied. Otherwise, the input is absent. The confidence interval can be obtained from the cumulative normal distribution table for a certain preset confidence level $1-\alpha^{10}$.

Once the input is estimated, the EKF is corrected with the estimated input at the same time. By incorporating the on-line input estimator into the EKF, the predicted and updated states at time interval $k\Delta t \leq t \leq (k+s)\Delta t$ are given by

$$\begin{aligned}\hat{X}^v(k+1|k+l-1) &= \phi(k+l-1)\hat{X}^v(k+l-1|k+l-1) \\ &\quad + \varphi_{\Delta}\hat{u}(k+l-1)\end{aligned}\quad (22)$$

$$\begin{aligned}\hat{X}^v(k+l|k+l) &= \hat{X}^v(k+l|k+l-1) + K^v(k+l) \\ &\quad [Z(k+l) - \hat{X}^v(k+l|k+l-1)]\end{aligned}\quad (23)$$

The Kalman gain becomes

$$K^v(k+l) = P^v(k+l|k+l-1)[P^v(k+l|k+l-1) + R]^{-1}\quad (24)$$

with the covariance matrices at $k\Delta t \leq t \leq (k+s)\Delta t$ being

$$\begin{aligned}P^v(k+l|k+l-1) &= P(k+l|k+l-1) \\ &\quad + \phi(k+l-1)L(k+l)\phi^T(k+l-1) \\ &\quad + \varphi_{\Delta}V(k+l-1)\varphi_{\Delta}^T\end{aligned}\quad (25)$$

$$P^v(k+l|k+l) = [I - K^v(k+l)]P^v(k+l|k+l-1)\quad (26)$$

where

$$\begin{aligned}L(k+l) &= 0 & L(k+2) &= N(k+2)V(k)N^T(k+2) \\ L(k+1) &= M(k+l-1)L(k+l-1)M_k^T(k+l-1)\end{aligned}$$

For time beyond the interval $t < k\Delta t$ and $t > (k+s)\Delta t$, state estimation can be also based upon the original EKF. Note that the initial states and covariance matrices at $t > (k+s)\Delta t$ are reinitiated by $\hat{X}^v(k+s|k+s)$ and $P^v(k+s|k+2)$. Figure 2 schematically depicts the proposed filter.

At $t > t_s$, measurement Z_i is sensed. The estimated input \hat{u}_i is then calculated using Eqn. (21) if Z is replaced by Z_i . Substituting \hat{u}_i into Eqns. (22) and (23) yields the predicted and updated states $\hat{X}_i^v(k+l|k+l-1)$, $\hat{X}_i^v(k+l|k+l)$ for the i -th object.

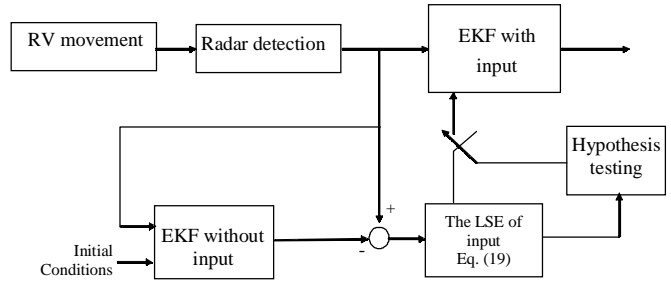


Figure 2. The mechanism of the proposed filter scheme.

4. IDENTIFICATION ALGORITHM

The MPDAF with the EKF and IE was presented to identify the warhead between two objects separation from the RV in a clear environment¹⁹ with clutter free. The major difference between MPDAF and the original PDAF is that the MPDAF considers the two real objects being tracked, but not random clutter. This section defines an algorithm associated with the MPDAF to track the warhead among N measured objects when $t > t_s$.

The proposed method comprises two steps. Selecting two candidates from N objects based on a certain criterion is the first, and then the MPDAF is used to compute the combined updated state from these two candidates.

4.1 Selection of Candidates

Assume N objects to be detected by a phased array radar with detection probability 1 during $t > t_s$. The predicted and updated states of the i -th object using the EKF with IE are, respectively,

$$\hat{X}_i^v(n+1|n) = \phi(n+1)\hat{X}_i^v(n|n) + \varphi_{\Delta}\hat{u}_i(n)\quad (27)$$

$$\begin{aligned}\hat{X}_i^v(n+1|n+1) &= \hat{X}_i^v(n+1|n) + K_i^v(n+1) \\ &\quad [Z_i(n+1) - \hat{X}_i^v(n+1|n)]\end{aligned}\quad (28)$$

with covariance matrices $P_i^v(n+1|n)$.

For more accurate choosing candidates, residual based on the updates states is adopted. Define the measurement residual of object i at $t = (n+1)\Delta t$ as

$$v_i(n+1) = Z_i(n+1) - \hat{X}_i^v(n+1|n+1)\quad (29)$$

Increasing the accuracy of the model reduces the distance between the measurement and predicted state in position. Restated, if the i -th object measurement $Z_i(n+1)$ is the target-originated measurement, then the length of the normalised residual in position is the smallest among all objects. Two candidates are chosen who are with the smallest values of the length of the normalised residual in position among N objects. These two candidates are sent to the MPDAF to calculate the association probabilities and combined updated state.

4.2 The MPDAF

Two candidates are selected based on the normalised residual defined in Eqn. (29). The MPDAF needs to compute the combined state from these two objects which may contain the warhead or just body and debris. Let $\hat{X}_{c1}^v(n+1|n+1)$ and

$\hat{X}_{c_2}^v(n+1|n+1)$ to be the updated states of two candidates corresponding to measurements $Z_{c_1}(n+1)$ and $Z_{c_2}(n+1)$, respectively, at time $t = (n+1)\Delta t$. Define the events to be

$$\theta_1(n+1) = \{ Z_{c_1}(n+1) \text{ is the target-originated measurement} \} \quad (30)$$

$$\theta_2(n+1) = \{ Z_{c_2}(n+1) \text{ is the target-originated measurement} \} \quad (31)$$

with association probabilities conditioned on Z^{n+1}

$$\beta_i(n+1) = \Pr\{\theta_i(n+1) | Z^{n+1}\} \quad i = 1, 2 \quad (32)$$

The association probabilities should satisfy

$$\beta_1(n+1) + \beta_2(n+1) = 1 \quad (33)$$

The updated state for the EKF with input estimation at time $t = (n+1)\Delta t$ can be regarded as

$$\hat{X}^v(n+1|n+1) = E[X(n+1) | Z^{n+1}] \quad (34)$$

Using the total probability theorem, $\hat{X}^v(n+1|n+1)$, known as the combined updated state, becomes¹⁶

$$\begin{aligned} E[X(n+1) | Z^{n+1}] &= E[X(n+1) | \theta_1(n+1) | Z^{n+1}] \\ &\Pr\{\theta_1(n+1) | Z^{n+1}\} + E[X(n+1) | \theta_2(n+1), Z^{n+1}] \\ &\Pr\{\theta_2(n+1) | Z^{n+1}\} \end{aligned} \quad (35)$$

then one gets

$$\begin{aligned} \hat{X}^v(n+1|n+1) &= \beta_1(n+1)\hat{X}_{c_1}^v(n+1|n+1) \\ &+ \beta_2(n+1)\hat{X}_{c_2}^v(n+1|n+1) \end{aligned} \quad (36)$$

The problem then focuses on the determination of β_i by means of Z_i .

As previously mentioned, trajectory of the warhead is closer to the original than of the body and debris. The innovations of the warhead are smaller than of other objects if an accurate estimation method is adopted. The larger association probability should be assigned to an object whose innovation is the smaller one between two objects. Thus, the association probabilities of the i -th object is inversely proportional to its length of the normalized innovation in position and can be defined as¹⁹

$$\beta_1(n+1) = \frac{e_2}{e_1 + e_2} \quad (37)$$

$$\beta_2(n+1) = \frac{e_1}{e_1 + e_2} \quad (38)$$

where e_i is the length of the normalised innovation in position for the i -th candidate. Substituting Eqns. (37) and (38) into Eqn. (36) yields the combined updated state of the object in track at $t=(n+1)\Delta t$. This estimated trajectory should be close to the warhead trajectory, such that the radar beam covers the warhead to maintain the track. Figure 3 shows the flow chart of the proposed algorithm combining the EKF with IE and the identification algorithm.

5. SIMULATION ANALYSIS

The performance of the proposed algorithm was evaluated

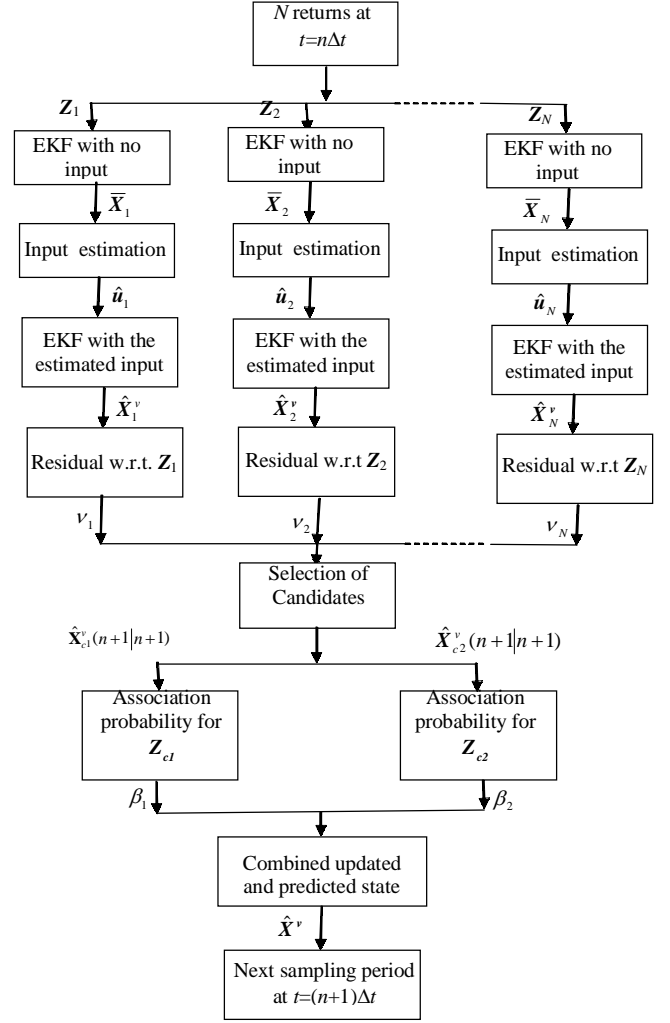


Figure 3. Flowchart of the proposed algorithm.

by inspecting the estimation error wrt the warhead, which signifies the difference between the estimated and actual warhead trajectories. The proposed algorithm should have a small estimation error w.r.t. the warhead to ensure that the warhead is constantly tracked. IE plays an important role in the proposed algorithm that provides accurate residuals. To indicate the importance of IE to tracking problem, the simulation results of the proposed algorithm were compared with those of the EKF with identification algorithm only. Denote the proposed algorithm as Method I and the EKF with the identification algorithm but without IE as Method II. The following study cases are with $N_{MC} = 50$ Monte Carlo runs.

Consider an RV in the reentry phase with $C = 2500 \text{ kg/m}^2$ and initial values of $x(0) = 300 \text{ m}$, $y(0) = 300 \text{ m}$, $z(0) = 30500 \text{ m}$, $v(0) = 1500 \text{ m/s}$, $\gamma_1(0) = 65^\circ$, and $\gamma_2(0) = 15^\circ$. The RV separates into the warhead, body, and two debris with the ballistic coefficients $C_1 = 2000 \text{ kg/m}^2$, $C_2 = 3000 \text{ kg/m}^2$, $C_3 = 3500 \text{ kg/m}^2$ and $C_4 = 4000 \text{ kg/m}^2$, respectively, at $t_s = 5 \text{ s}$. Equations (1) ~ (9) simulate the trajectories of the warhead, body, two debris, and the original RV without separation. Measurement noises are generated by following the standard normal distribution. Figures 4 to 9 display the measured trajectories with measurement noises. The

sampling period of the radar is $\Delta t = 0.1$ s. The flight times of the original RV, warhead, body, and two other debris are 36 s, 42 s, 33 s, 31 s, and 29 s, respectively. The body and two debris are falling down faster than the warhead. The purpose of the proposed algorithm is to identify the warhead among these four objects.

The ballistic coefficient was set to a constant of $C = 2500$ kg/m² in entire estimation. Let the confidence level $1-\alpha$ to be 0.95. The initial conditions of R , Q , V , and $P^v(0|0)$ were $I_{6 \times 6}$, $I_{6 \times 6}$, $500I_{6 \times 6}$, and $500I_{6 \times 6}$, respectively. R and Q remain constants in entire estimation. The first detection $Z(0)$ is taken as initial state $\hat{X}^v(0|0)$.

Figures 10 and 11 show the relative association probability evolution by Methods I and II, respectively. The association probability of Method I for the warhead reached 1 within 2s. Restated, the estimated trajectory followed the warhead, and was never affected by the measurements of the body and debris in 2s after separation. However, Method II assigned the same probabilities to the warhead and another object. The radar beam

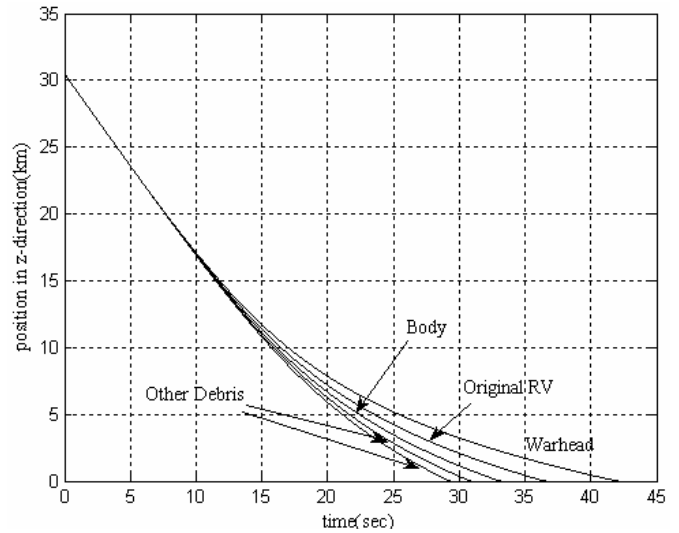


Figure 6. The measured position of objects in altitude.

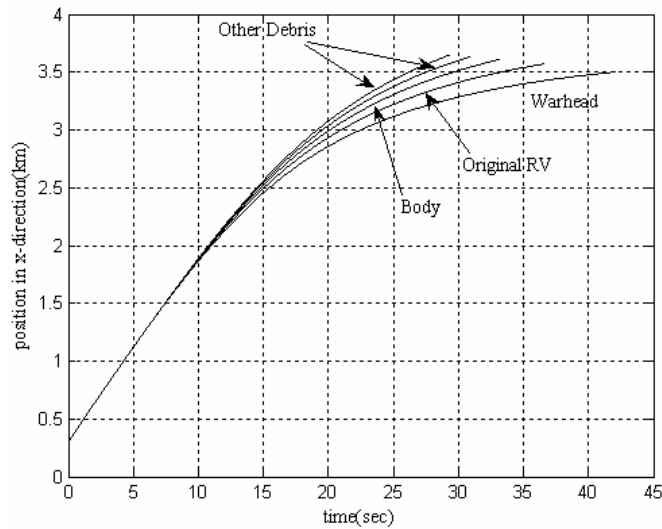


Figure 4. The measured position of objects in downrange.

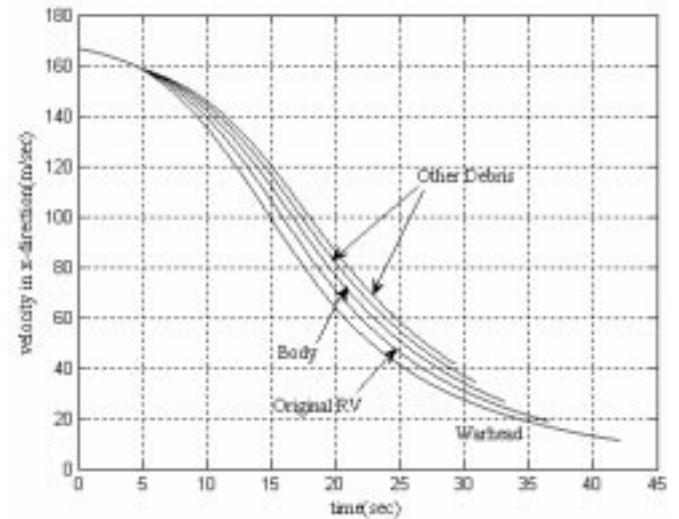


Figure 7. The measured velocity of objects in X_R .

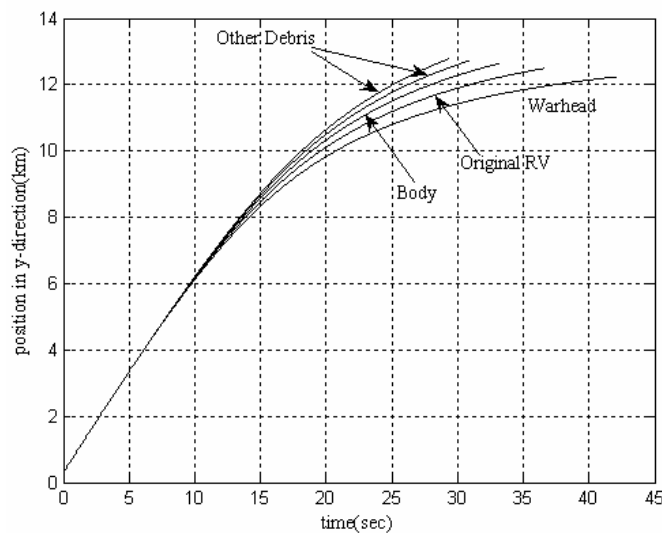


Figure 5. The measured position of objects in offrange.

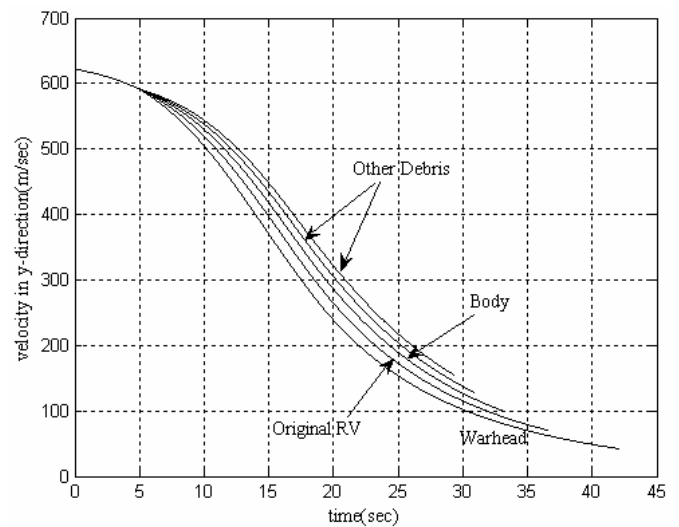


Figure 8. The measured velocity of objects in Y_R .

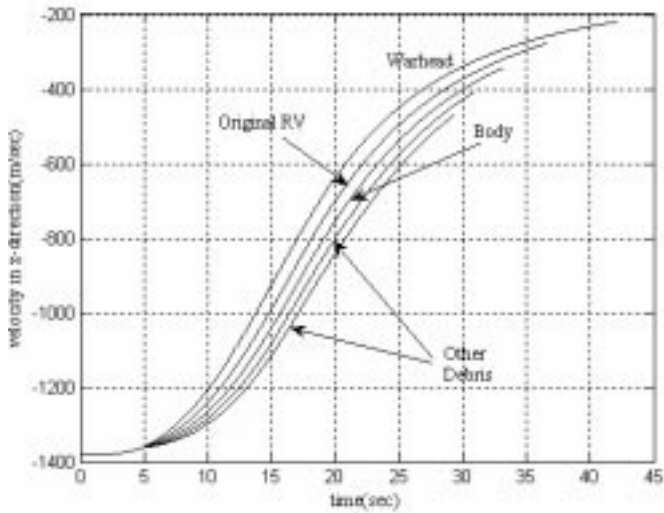


Figure 9. The measured velocity of objects in Z_R .

thus denoted the location with the same distance to warhead as to another object. This implies that the radar lost the track if all objects have a large enough separating distance. Figure 12 shows the norms of estimation error for Method I wrt. the warhead. The error norms induced by Method I were limited to 5m in position and 9 m/s in velocity. The small estimation error ensures that the warhead located in the radar beam and was tracked all the time. The body and two debris were thus no longer in the same radar beam. Figure 13 displays the norm of the estimation error generated by Method II w.r.t. the warhead that were almost up to 1500m in position and 450m/s in velocity and larger than those induced by Method I. Figures 14 -17 depicts the standard deviations (SD's) of the estimated position and velocity for Methods I and II that converged to an acceptable range in a certain time. The SD of Method I was slight greater than those of method II because of involvement of IE.

Case 1: Maneuvering Warhead:

Maneuvering is generally undertaken after separation to

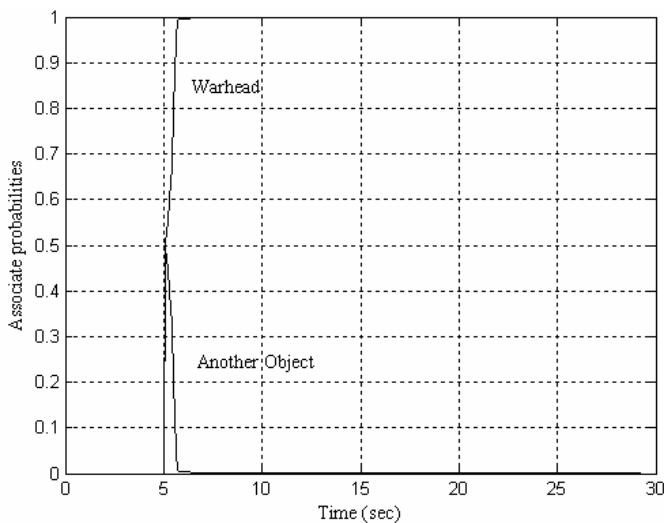


Figure 10. Association probabilities of warhead and other objects for Method I.

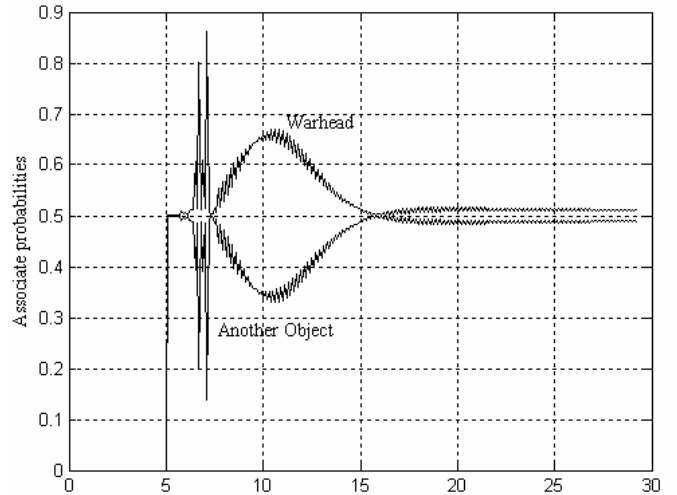


Figure 11. Association probabilities of warhead and other objects for Method II.

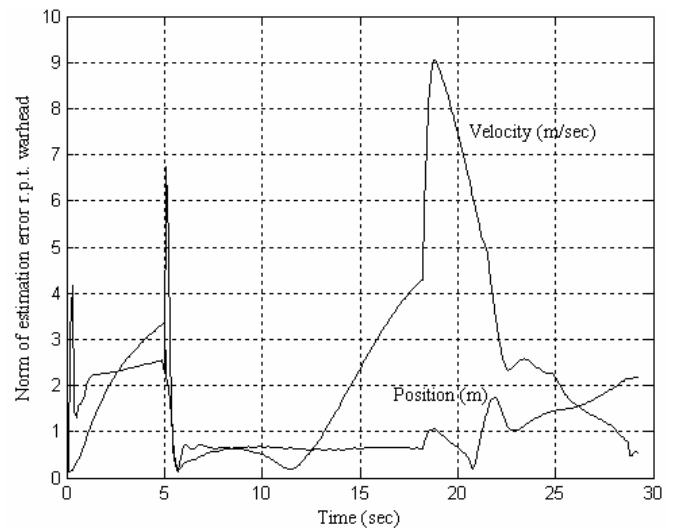


Figure 12. Norm of estimation errors wrt the warhead for Method I.

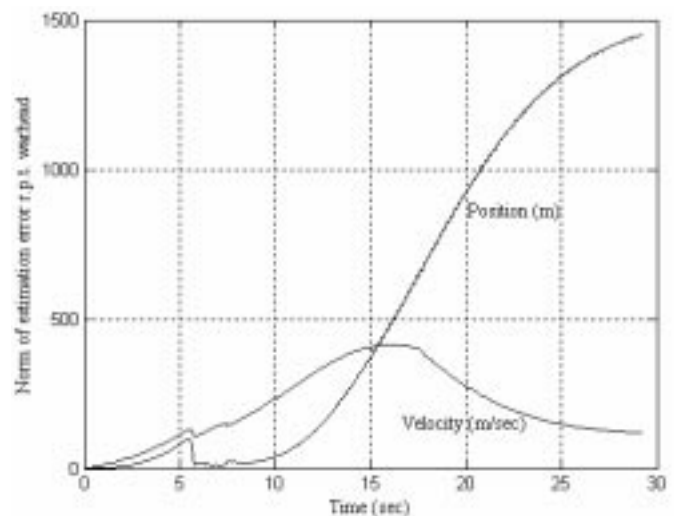


Figure 13. Norm of estimation errors wrt the warhead for Method II.

change warhead trajectory. Consider the case that 3G, 3G, and -3G lateral accelerations with duration 3 s along three axes at 2 s after separation are undertaken by the warhead. Figures 18 and 19 show the corresponding association probability evolution formed by methods I and II, respectively. The association probability of method I to warhead reached 1 in 2 s as in the nonmanoeuvring case, but fluctuated after maneuvering, and died out rapidly after termination. Nevertheless, method II gives the same probabilities to the warhead and another object as the nonmaneuvering case. The proposed algorithm assigned higher probabilities to the warhead than to another object that led the radar to track the warhead as well as the nonmaneuvering case. The IE estimates the unknown input terms and helps identification algorithm to select the right target and keep in track. Figure 20 demonstrates the norms of estimation error for Method I that were restricted to 27 m in position and 5 m/s in velocity. The small error made the radar to track warhead well. Figure 21 shows the norms produced by method II that were much larger than those produced by method I. Figures 22~25 depict the SD's of these two methods that both converged to a certain interval. This case measures the robustness property of Method I to model error generated by maneuvering.

Case 2: Parameter Uncertainty:

This case evaluates the robustness of the proposed algorithm to ballistic coefficient, initial values of state and its covariance, and confidence level by inspecting the root mean square (RMS) of estimation error for real time. The RMS is defined as²³

$$RMS = \frac{1}{N_{MC}} \sum_{j=1}^{N_{MC}} \left\{ \frac{1}{N_p} \sum_{i=1}^{N_p} [v_j(i) - \bar{v}_j(i)]^T [v_j(i) - \bar{v}_j(i)] \right\} \quad (39)$$

where $v_j(i)$ and $\bar{v}_j(i)$ denote the estimation error and its mean, respectively, at the j -th run and N_p is the total number of samples.

The ballistic coefficient is the critical parameter for the RV dynamic equations and is unknown for the defender. One

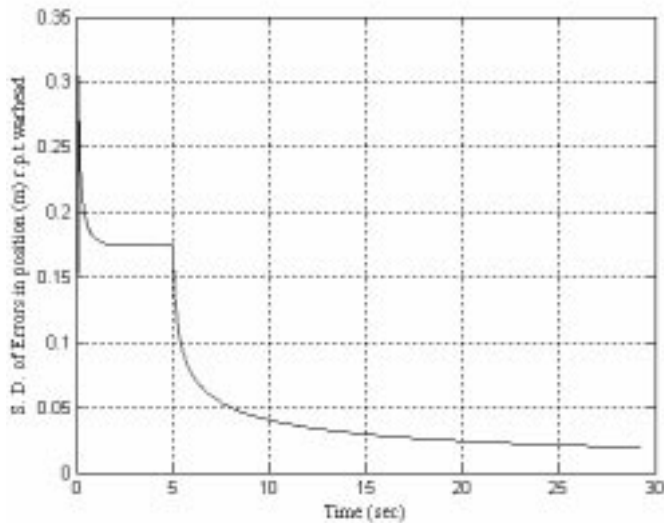


Figure 14. SD of errors in position wrt the warhead for Method I.

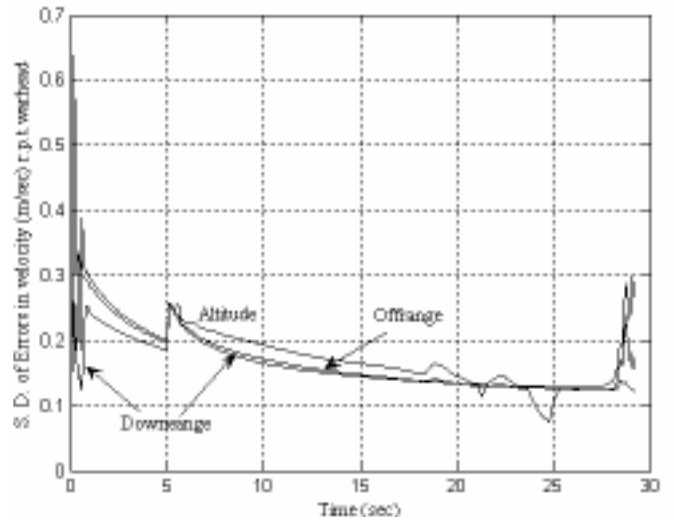


Figure 15. SD of errors in velocity wrt the warhead for Method I.

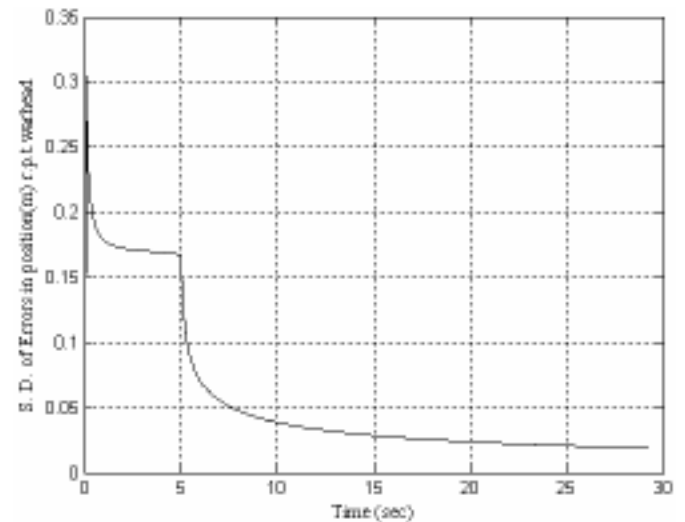


Figure 16. SD of errors in position wrt the warhead for Method II.

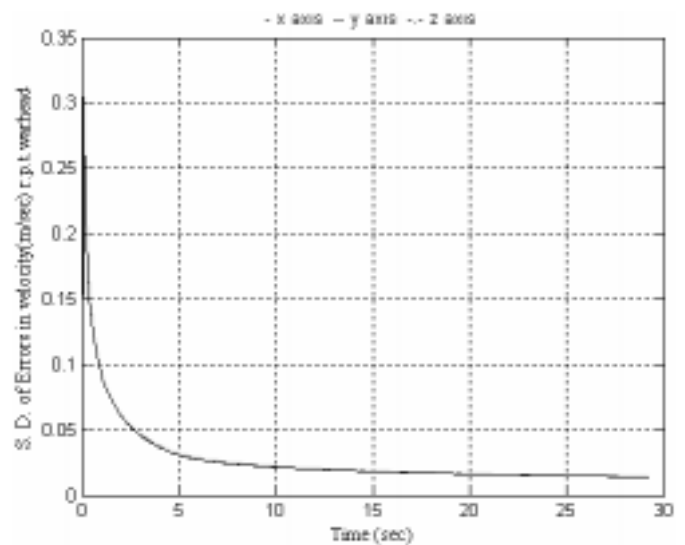


Figure 17. SD of errors in velocity wrt the warhead for Method II.

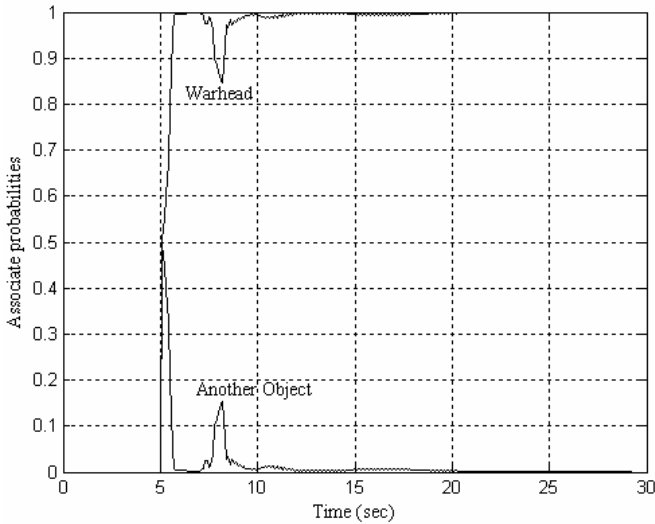


Figure 18. Association probabilities for Method I under manoeuvring case.

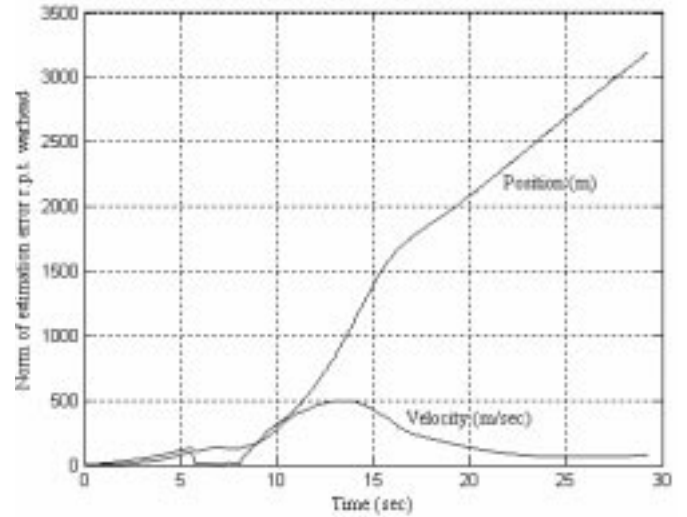


Figure 21. Norm of estimation errors wrt the warhead for Method II under manoeuvring case.

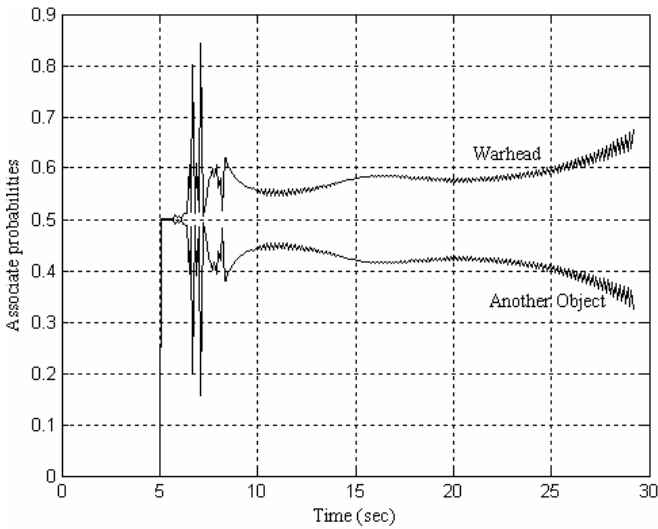


Figure 19. Association probabilities for Method II under manoeuvring case.

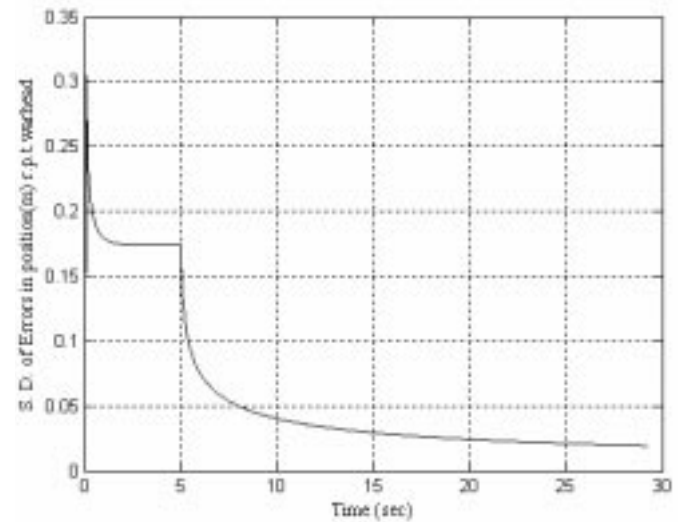


Figure 22. SD in position wrt the warhead for Method I under manoeuvring case.

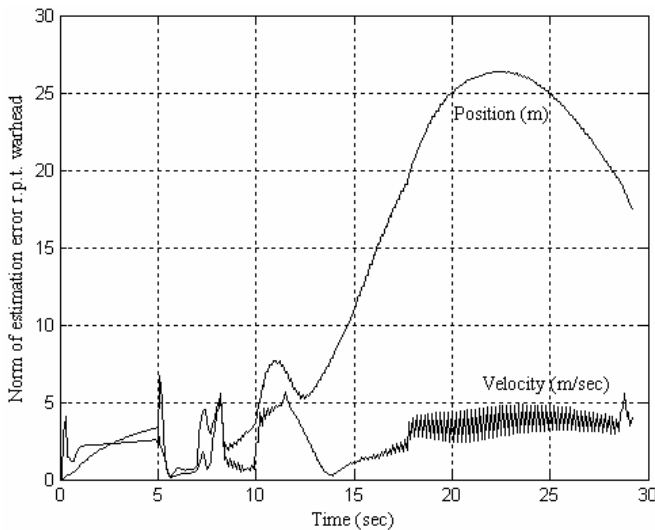


Figure 20. Norm of estimation errors wrt the warhead for Method I under manoeuvring case.

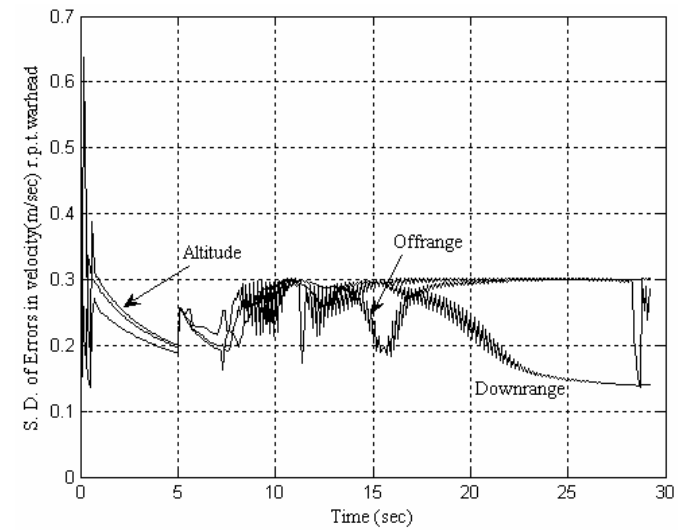


Figure 23. SD in velocity wrt the warhead for Method I under manoeuvring case.

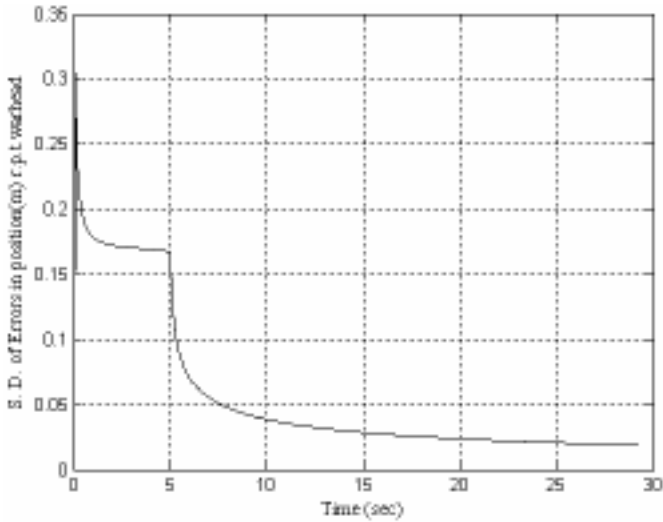


Figure 24. SD in position wrt the warhead for Method II under manoeuvring case.

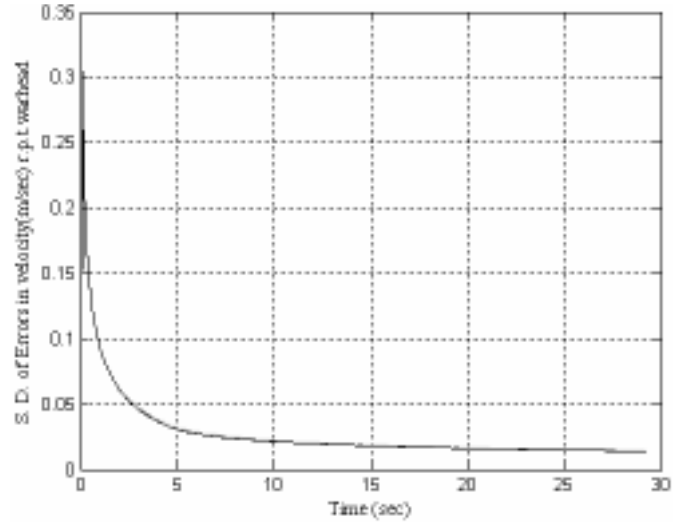


Figure 25. SD in velocity wrt the warhead for Method II under manoeuvring case.

should assign a constant to the ballistic coefficient before estimating and tracking. If the assigned ballistic coefficient is far away from the true value, the model error increases and the estimated trajectory might become unreliable. Table 1 lists the RMS of estimation errors for non-manoevring and manoeuvring cases in different assigned ballistic coefficients. This indicates that only a little change for mehtod I was achieved and confirms that the proposed approach is robust to the ballistic coefficient.

Tables 2 and 3 summarise the RMS of estimation error induced by varying initial state and covariance, respectively. For initial state, the estimation errors produced by Method I were larger than the original especially in Z_R . Taking $Z(0)$ as an initial is simple and is suggested. From Table 3, Method I provided a slight difference and an acceptable errors due to $P^v(0|0)$ variation. Although Method II also had a slight change, its estimation errors were unacceptable. Covariance of process noise, Q , is another critical parameter for EKF. Q is assigned to be a constant matrix in entire estimation procedure for both non-manoevring and manoeuvring cases. Table 4 lists the RMS

for methods I and II in different Q . The RMS's for method I were small and almost the same. However, the RMS's offered by method II were much greater than those by mehtod I. According to these two tables, robustness of the proposed algorithm to $P^v(0|0)$ and Q was validated.

Confidence level relates input duration l and confidence interval means a threshold to detect inputs during estimation. Lower confidence level, implying larger l , allows more estimated inputs to join into the estimation procedure. Table 5 summarises the RMS of estimation error generated by Method I for different confidence levels or window lengths. The RMS's were almost the same for cases of confidance levels 0.9, 0.85, and 0.8. This reveals that the proposed method is robust to confidence level because errors induced by unreal inputs can be corrected by the estimated input at next sampling period.

6. CONCLUSIONS

This study presents an accurate algorithm for tracking a warhead that has separated from a reentry vehicle in the reentry

Table 1. RMS of the estimation error for non-manoevring (above) and manoeuvring (below) cases in different assigned C

Assigned C (kg/m ²)	Position in X_R (m)	Position in Y_R (m)	Position in Z_R (m)	Velocity in X_R (m/s)	Velocity in Y_R (m/s)	Velocity in Z_R (m/s)
1500	1.09 (754.16)*	1.12 (227.03)	1.4 (1677.2)	0.91 (188.8)	1.98 (123.5)	4.14 (180.09)
	3.33 (830.53)	9.66 (352.49)	13.02 (1522.6)	1.83 (255.91)	1.52 (147.15)	4.42 (323.89)
3500	0.56 (300.07)	0.53 (27.63)	0.85 (567.75)	0.54 (105.72)	1.17 (100.46)	2.28 (125.79)
	3.64 (301.31)	8.54 (235.52)	12.86 (573.62)	1.24 (95.31)	1.06 (83.87)	2.93 (187.4)
5000	0.46 (346.73)	0.46 (506.42)	0.79 (1587.8)	0.48 (89.3)	1.04 (108.71)	1.97 (163.55)
	6.16 (309.94)	10.64 (136.73)	10.15 (1704.1)	0.92 (106.22)	1.24 (56.64)	2.23 (169.02)

* Value in (.) means the RMS from Method II.

phase. The proposed method comprises an extended Kalman filter, an input estimator, and an identification algorithm. The extended Kalman filter associated with input estimation can accurately predict the trajectory. The identification algorithm

selects candidates and offers a precision combined updated state for the warhead from all measured objects. Simulation results monitor the performance of the recommended method by inspecting the estimation error corresponding to the warhead,

Table 2. RMS of the estimation error for non-manoeuving (above) and manoeuvring (below) in initial state variation

$\hat{X}^v(0 0)$	Position in X_R (m)	Position in Y_R (m)	Position in Z_R (m)	Velocity in X_R (m/s)	Velocity in Y_R (m/s)	Velocity in Z_R (m/s)
0.5Z(1)	8.94 (456.25)*	8.94 (96.02)	890.33 (1078.4)	4.91 (148.21)	18.23 (121.1)	40.4 (201.15)
	10.51 (234.92)	10.27 (209.4)	890.44 (1898.6)	5.05 (105.46)	18.25 (43.14)	40.44 (151.46)
2Z(1)	17.83 (457.39)	17.83 (97.07)	1780.7 (1882.2)	9.75 (148.66)	36.37 (125.29)	80.75 (168.65)
	19.3 (192.69)	18.81 (278.27)	1780.8 (1800.7)	9.83 (114.58)	36.42 (98.24)	80.77 (166.9)

* Value in (.) means the RMS from Method II.

Table 3. RMS of the estimation error for nonmanoeuvring (above) and manoeuvring (below) in different initial covariance

$P^v(0 0)$	Position in X_R (m)	Position in Y_R (m)	Position in Z_R (m)	Velocity in X_R (m/s)	Velocity in Y_R (m/s)	Velocity in Z_R (m/s)
$10I_{6 \times 6}$	0.69 (457.39)*	0.67 (95.95)	0.95 (609.63)	0.64 (148.52)	1.38 (120.04)	2.78 (146.2)
	2.93 (830.53)	8.96 (352.49)	12.42 (1522.6)	1.08 (255.91)	1.05 (147.15)	2.97 (323.89)
$100I_{6 \times 6}$	0.67 (456.57)	0.67 (95.61)	0.95 (609.01)	0.65 (148.24)	1.38 (119.82)	2.77 (146.05)
	3.22 (233.61)	8.97 (210.17)	12.76 (1676.6)	1.08 (105.69)	1.21 (38.57)	2.62 (197.83)
$1000I_{6 \times 6}$	0.69 (456.48)	0.67 (95.58)	0.95 (608.9)	0.64 (148.21)	1.39 (119.79)	2.76 (146.04)
	10.87 (234.32)	7.51 (210.05)	28.4 (1677.0)	1.02 (105.62)	2.79 (38.79)	3.38 (197.65)

* Value in (.) means the RMS from Method II.

Table 4. RMS of the estimation error for non-manoeuving (above) and manoeuvring (below) in different Q

Q	Position in X_R (m)	Position in Y_R (m)	Position in Z_R (m)	Velocity in X_R (m/s)	Velocity in Y_R (m/s)	Velocity in Z_R (m/s)
$0.3I_{6 \times 6}$	0.7 (512.07)*	0.68 (213.98)	0.92 (1292.9)	0.65 (135.51)	1.39 (112.55)	2.77 (155.14)
	2.93 (225.92)	8.96 (207.82)	12.42 (1670.3)	1.08 (105.43)	1.05 (38.92)	2.97 (193.58)
$3I_{6 \times 6}$	0.69 (140.25)	0.67 (132.59)	0.96 (453.38)	0.64 (105.01)	1.39 (105.58)	2.76 (139.45)
	3.22 (304.45)	8.97 (259.71)	12.76 (1375.3)	1.08 (78.92)	1.21 (63.22)	2.62 (179.12)
$10I_{6 \times 6}$	0.69 (168.01)	0.67 (558.22)	0.95 (1380.4)	0.64 (81.28)	1.39 (93.38)	2.76 (140.72)
	10.87 (344.5)	7.51 (133.14)	28.4 (692.76)	1.02 (94.62)	2.79 (39.45)	3.38 (219.07)

* Value in (.) means the RMS from Method II.

Table 5. RMS of estimation error induced by method I for non-maneuvring (above) and manoeuvring (below) in different confidence levels

$1-\alpha$ (t_{α})	Position in X_R (m)	Position in Y_R (m)	Position in Z_R (m)	Velocity in X_R (m/sec)	Velocity in Y_R (m/sec)	Velocity in Z_R (m/sec)
0.9 (1.64)	0.7 3.12	0.68 8.99	0.96 12.76	0.64 1.07	1.39 1.11	2.78 2.79
0.85 (1.44)	0.7 3.46	0.68 8.91	0.96 13.09	0.64 1.21	1.39 1.2	2.8 2.7
0.8 (1.28)	0.7 3.63	0.68 8.96	0.96 12.83	0.64 1.25	1.39 1.29	2.8 2.54

which should be minimised. Robustness of the proposed algorithm to critical parameters in the model is also evaluated by simulation. This investigation thus concludes that the proposed algorithm is worthy of further study and applications. The effects of a nonlinear measurement equation, when a filter for estimating velocity is involved, will be concerned. Ballistic coefficient estimation is another future study issue for increasing the accuracy more.

ACKNOWLEDGMENT

The authors would like to thank the National Science Council of the Republic of China for financially supporting this research under Contract No. NSC 96-2221-E-234-001.

REFERENCES

- Chan, Y. T.; Hu, A. G. C. & Plant, J. B. A Kalman filter based tracking scheme with input estimation. *IEEE Trans. Aerosp. Electro. Syst.*, 1979, **AES-15**, 237-44.
- Chan, Y. T.; Plant, J. B. & Bottomley, J. A Kalman tracker with a simple input estimator. *IEEE Trans. Aerosp. Electro. Syst.*, 1982, **AES-18**, 235-41.
- Bogler, P. L. Tracking a maneuvering target using input estimation, *IEEE Trans. Aerosp. Electro. Syst.*, 1987, **AES-23**, 298-310.
- Tuan, P. C. & Fong, L. W. An IMM tracking algorithm with input estimation, *Int. J. Syst. Sci.*, 1996, **27**, 629-39.
- Tuan, P. C.; Ji, C. C. ; Fong, L. W. & Huang, W. T. An input estimation approach to on-line two-dimensional inverse heat conduction problem. *Numeri. Heat Transfer; Part B*, 1996, **29**, 345-63.
- Chen, T. C. & Tuan, P. C. Inverse problem of estimating interface conductance between periodically contacting surface using the weighting input estimation method. *Numeri. Heat Transfer; Part B*, 2002, **41**, 477-92.
- Chen, T. C. & Tuan, P. C. Input estimation method including finite element scheme for solving heat conduction problems. *Numeri. Heat Transfer; Part B*, 2005, **47**, 277-90.
- Lee, S. C. & Liu, C. Y. Fast automatic leveling subject to abrupt deterministic input, *IEEE Trans. Aerosp. Electro. Syst.* 1999, **AES-35(3)**, 989-96.
- Lee, S. C.; Liu, C. Y. & How, W.T. Initial leveling with input estimation. *JSME Inter. J., Series C*, 1998, **41(4)**, 724-80.
- Lee, S. C. & Liu, C. Y. Trajectory estimation of reentry vehicles by use of on-line input estimation. *J. of Guid. Control Dyn.*, 1999, **22**, 808-15.
- Lee, S. C.; Huang, Y. C. & Liu, C. Y. Trajectory estimation for tactical ballistic missile in terminal phase using on-line input estimator. *Proc. Natl. Counc. ROC(A)*, 1999, **23(5)**, 644-53.
- Chi, P. H. & Liu, C. Y. Novel on-line trajectory estimation of a reentry vehicle. *Trans. Aero.Astro. Soc. Republic of China*, 2000, **32(4)**, 291-300.
- Liu, C. Y., Wang, H. M. & Tuan, P. C. Input estimation algorithms for reentry vehicle trajectory estimation, *Def. Sci. J.*, 2005, **55(4)**, 361-75.
- Liu, C. Y., Liu, C. C. & Tuan, P. C. Algorithm of impact point prediction for intercepting reentry vehicles, *Def. Sci. J.*, 2006, **56(2)**, 129-46.
- Bar-Shalom, Y. & Tse, E. Tracking in a cluttered environment with probabilistic data association. *Automatica*, 1975, **11**, 451-60.
- Bar-Shalom, Y. & Fortmann, T.E., Tracking and data association. Academic Press Inc, 1988.
- Fortmann, T. E.; Bar-Shalom, Y. & Scheffe, M. Sonar tracking of multiple targets using joint probabilistic data association, *IEEE J. Oceanic Engi.*, 1983, **8(3)**, 173-84.
- Chen, B. & Tugnait, J. K. Tracking of maneuvering targets in clutter using imm/jpda filtering and fixed-log smoothing, *Automatica*, 2001, **37**, 239-49.
- Liu, C. Y. & Sung, Y. M. Clarifying warhead separation from the reentry vehicle using a novel tracking algorithm, *Inter. J. Control Auto. Syst.*, 2006, **4(5)**, 529-38.
- Zarchan, P. Tactical and Strategic Missile Guidance, American Institute of Aeronautics and Astronautics Inc, 1994.
- Siouris, G. M. Aerospace avionics system: A modern synthesis. Academic Press Inc., 1993.
- Gelb, A. Applied optimal estimation. The M.I.T. Press, MA, 1974.
- Bar-Shalom, Y.; Li, X. R., & Kirubarajan, T. Estimation with applications to tracking and navigation. John-Wiley & Sons, Inc, 2001.

Contributors



Dr Cheng-Yu Liu received his MS and PhD both from Chung Cheng Institute of Technology Taiwan, in 1983 and 1998, respectively. He worked at the Chung Shan Institute of Science and Technology during 1985-2002. Presently, he is Associate Professor in the Department of Electronic Engineering of the Lee-Ming Institute of Technology. His research areas include system identification, control theory, and tracking system.



Dr Chi-Teh Chen received his MS and PhD both from Chung Cheng Institute of Technology, Taiwan, in 1985 and 1999, respectively. He worked at the 202 Arsenal of Combined Service Forces ROC from 1985 to 2001. Presently, he is Assist Professor in the Department of Electronic Engineering of the Lee-Ming Institute of Technology. His research area includes signal processing, guidance and control, and estimation theory.